Emerging hyper-fluorescent emitters for solid-state lighting

Santosh Kumar Behera[1]* and Rubén D. Costa[1]*

[1]Chair of Biogenic Functional Materials, Technical University of Munich, Campus Straubing for Biotechnology and Sustainability, Schulgasse 22, D-94315 Straubing, Germany.

*Corresponding authors: SKB (Email: santoshbeherau@gmail.com) and RDC (Email. *ruben.costa@tum.de*)

Abstract: Organic light-emitting diodes (OLEDs) are of high interest for display, biomedical, and solid-state lighting applications. But, costs and color purity are still issues with OLED technology. The development of triplet harvesting emitters with a thermally activated delayed fluorescence (TADF) mechanism mends these problems to some extent, owing to their ability to produce both singlet and triplet excitons. In addition, the recent development of hyperfluorescent OLEDs (HF-OLED) based on TADF and fluorescence emitter couples have attracted a lot of attention, realizing high efficiency, good stability, and narrow emission. In this mini-review, we comprehensively documented the molecular design principles of hyperfluorescence emitters, their fundamental photophysics, and the advances in their applications in OLEDs. Finally, the future perspectives of hyperfluorescence emitters and OLEDs are envisaged.

Keywords: organic emitter, hyper-fluorescence, Förster resonance energy transfer, thin-film lighting and white light emission.

1. Introduction

The fundamental development of new emitters for organic light-emitting diodes (OLEDs) has always grabbed a lot of attention.[1,2] Since they play an important role in developing efficient OLEDs in terms of color purity, efficiency, and stability; key aspects for applications in displays, biomedical, and solid-state lighting.[1-11] **Fig. 1a** displays the multilayered architecture of OLEDs and their mechanisms allowing direct charge injection, transport, and recombination to form emitting excitons.[7] According to the principle of spin statistics, the excitation of the emitter leads to the formation of 25% singlet excitons and 75% triplet excitons.[9] The emitters based on small molecules present in the active layers of OLEDs are broadly classified into three types, such as fluorescence, phosphorescence, and thermally activated delayed fluorescence (TADF) emitters (**Fig. 1b**).[1, 12-27] Their basic photophysical properties are well reported in many excellent reviews and literatures.[28-38] The first generation of OLEDs are based on fluorescent emitters (emission comes only from the S_1 state after excitation), which harvest only 25% of singlet excitons and therefore reach 25% of maximum internal quantum efficiency (IQE), since 75% of triplet excitons are dark. The external quantum efficiency (EQE) of an OLED device depends on IQE and relates to each other as follows: [9]

$$\eta_{EQE} = \eta_{IQE} \times \eta_{out} = \left(\gamma \times \eta_{\gamma} \times \Phi_{PL}\right) \times \eta_{out} \quad (1)$$

Where, η_{IQE} and η_{out}, denote the internal quantum efficiency and the light-out-coupling efficiency, respectively. Eq. 1 revealed that η_{IQE} depends on γ (charge balance factor of injected holes and electrons), η_{γ} (efficiency of radiative exciton production), and Φ_{PL} (photoluminescence quantum yield). In case of fluorescence emitters, η_{γ} is strongly limited, since the 75% of electrically generated dark triplet excitons. Therefore, there

was a search for techniques/emitters to harvest them, that is, the development of second and third generation of emitters. The Second generation of OLEDs are based on phosphorescent emitters (e.g., Iridium(III) and Platinum (II) complexes) that harvest both singlet and triplet excitons, reaching 100% of maximum η_{IQE}.[24,25,39-41] Though it overwhelms the limitations of conventional fluorescent OLEDs, its broad emission renders the poor color purity of the devices. In addition, sustainability and cost concerns are always present when using rare-earth materials. The third generation of OLEDs based on TADF organic emitters with a very small singlet-triplet energy gap (ΔE_{ST}), which produces both singlet and triplet excitons through an efficient triplet to singlet up-conversion process, enables them to reach 100% of η_{IQE}.[15] The TADF emitters significantly enhanced the OLED performance, promising low-cost and sustainable emitters. However, the wide emission spectra of TADF emitters still limit the low color purity of the devices, and the long-lived excitons are leading to degradation processes that reduce the η_{EQE} and device stability.

It is in this context that the hyperfluorescence (HF) emitters are emerging. Indeed, they have been referred to as the fourth generation on OLED active layers. [42-60] HF is defined as the emission mechanism that combines two different emitters, such as TADF and fluorescence emitters (**Fig. 1c**). As stated, TADF molecules have a small energy gap (ΔE_{ST}) between the singlet and the accepting triplet energy states. This permits the up-conversion of excited energy from accepting triplet to singlet states, which provides efficient emission from the singlet state.[31] However, if the excited energy produced by the TADF emitter is harvested by a fluorescent molecule following the Förster resonance energy transfer (FRET) process, this will emit four times more photons than conventional fluorescence at the same excitation conditions.[49] In addition, HF emitters display a strong and narrow-band emission, contrary to the broad emission of TADF

emitters. Therefore, HF has been established as a promising approach to designing OLEDs with high color purity and enhanced stability.[42-60] The study of HF emitters and their optoelectronic applications is progressing with momentum. In this mini-review, we systematically documented the molecular design principles of HF emitters, their fundamental photophysical requirements, and the advances in HF-OLED.

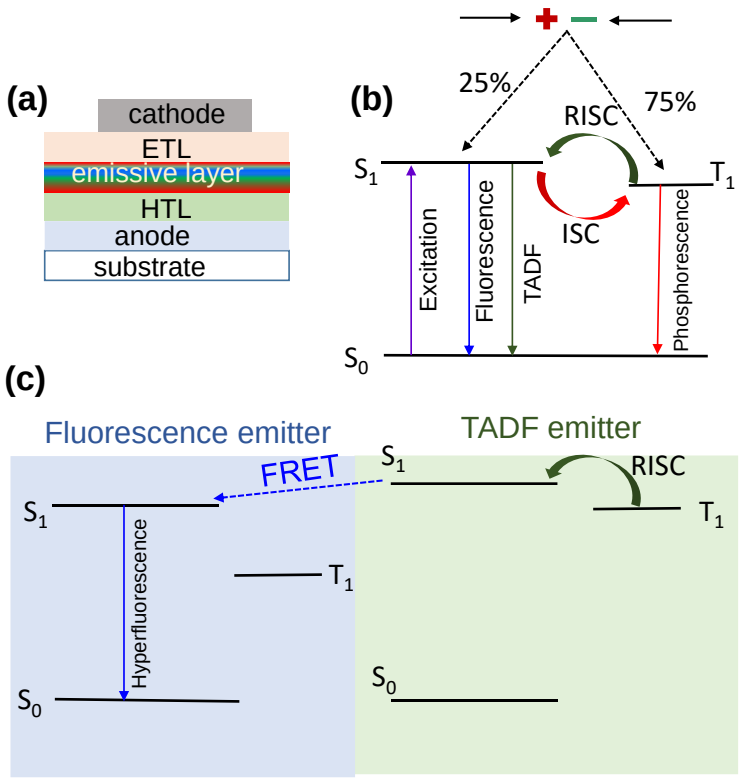

Fig. 1 (a) Multilayered architecture of OLEDs: Hole transport layer (HTL) and Electron transport layer (ETL); (b) Photophysical processes of different emitters; and (c) Mechanism of hyper-fluorescence with TADF sensitizer and fluorescence emitter.

2. Strategies for designing hyperfluorescent emitters

The emitting layer of HF-OLED contains a TADF emitter, a fluorescent emitter, and/or a host. Therefore, the design of each material is crucial (**Figs. 2-5**), which is briefly depicted as follows:

TADF emitter acts as a sensitizer, which plays an important role in harvesting the singlet excitons of fluorescence emitters. Therefore, the TADF emitters should have an

efficient RISC rate (k_{RISC}) from T_n to S_1. In addition, the TADF emitters should have a high Φ_{PL} in thin film. The fluorescent emitter must feature a high Φ_{PL} and a small Stokes' shift for efficient energy transfer. Furthermore, an efficient FRET (high k_{FRET}) process requires the maximum overlap between the absorption spectrum of the fluorescence emitter and the emission spectrum of the TADF emitter. Finally, the first singlet excited state (S_1) of the fluorescence emitter must be below that of the S_1 state of the TADF emitter (**Fig. 1c**). The concentration of two emitters is also crucial for efficient HF behavior. Typically, a doping strategy is followed, in which a high amount of TADF emitter and a lesser amount of fluorescence emitter in the active layer is required. Concerning the host material, it is required to feature higher energy (singlet and triplet) than the fluorescence and TADF emitters to prevent reverse energy transfer. Moreover, it is also very important to prevent Dexter energy transfer (DET) among triplet states to avoid loss of triplet exciton, which is achieved through efficient k_{RISC}, and the use of less doping concentrations of emitters. Finally, a key requirement is to control carrier trapping, which is essential to forbid the formation of triplet exciton in the dopant fluorescence emitter.[44,61]The implementation of bulkier groups in fluorescence emitter is the most suitable approach to control it. In the last few years, resonance (MR)-TADF terminal emitters have been greatly used in HF-OLEDs. Concerning the current use of MR-TADF terminal emitters, they should have short-range charge transfer characteristics, a small Stoke shift and efficient k_{RISc}.

Strategies for designing hyper-fluorescent emitters

- ✓ High k_{RISC} for TADF emitter
- ✓ High PLQY of fluorescence emitter
- ✓ High k_{FRET}
- ✓ $E_{S1\ level}$ (Fluorescence emitter) < $E_{S1\ level}$ (TADF emitter)
- ✓ Optimized doing concentrations ($C_{Fluorescence\ emitter} < C_{TADF\ emitter}$)
- ✓ Triplet energy of Host > Triplet energy of TADF emitter
- ✓ High k_{RISC} for MR-TADF terminal emitter

Fig. 2 Plausible conditions for designing of efficient hyper-fluorescent molecules.

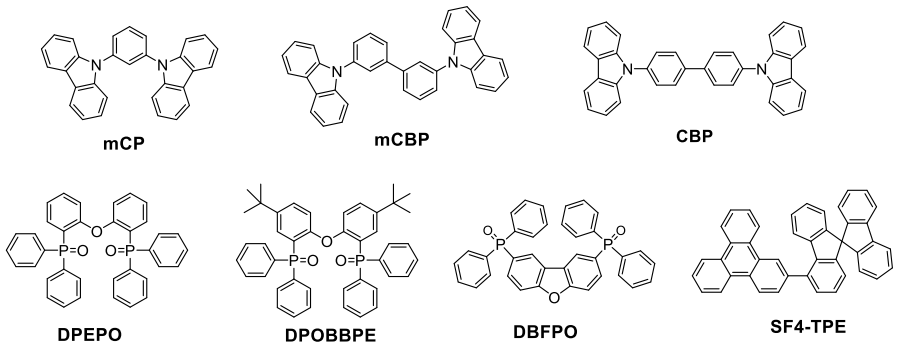

Fig. 3 Chemical structures of host materials.

The FRET processes are evaluated by using simple following mathematical equations:[53,56]

$$k_{\mathrm{FRET}} = \frac{1}{\tau_F}\left(\frac{R_0}{R}\right)^6 \quad (2)$$

where τ_F is the prompt fluorescence lifetime, R_0 is the Förster radius, at which the energy transfer efficiency is 50% and R denotes the average intermolecular distance between fluorescence dopant and TADF emitter.

$$R_0{}^6 = \frac{9000\Phi_F\kappa^2}{128\pi^5 n^4} J_F \quad (3)$$

where, n, κ^2 and Φ_F are the refractive index of the medium, dipole orientation factor, the prompt quantum yield of the TADF emitter, respectively.

$$J_F = \int F_D(\lambda)\epsilon_A(\lambda)\lambda^4 \, d\lambda \quad (4)$$

where, $F_D(\lambda)$ accounts the normalized emission spectrum of TADF emitter and $\epsilon_A(\lambda)$ accounts the molar extinction coefficient of the fluorescence dopant, respectively.

A few representative examples of successful TADF/fluorescence emitter combinations are described as follows: **F1** is one of the best fluorescence emitters used for the development of narrow-emitting HF-OLED (**Fig. 5**).[53,62,63] The emitter **F1/MR-T1** exhibits a strong absorption band at 457 nm and a sharp fluorescence band at 468 nm, with full width at half maximum (FWHM) of about 14 nm in toluene. This is related to the combined effect of its polycyclic structure and the multiple resonance (MR) effect of the boron and nitrogen atoms.[64] In addition, **F1** exhibits a Φ_{PL} of 74% in toluene. In fact, **F1** and its derivatives are also TADF active and recently been employed in many HF-OLED as terminal emitters with MR-TADF characteristics (discussed later). Therefore, a suitable TADF material with a close emission to that of the absorption spectrum of fluorescence emitter **F1/ MR-T1** is essential for the construction of an efficient HF device.

Kwon and co-workers selected TADF emitters **T_1** and **T_2** (**Fig. 4**); they contain an acceptor-donor-acceptor backbone with an oxygen-bridged boron acceptor, which usually resulted in a deep blue emission upon photoexcitation. Indeed, their emission

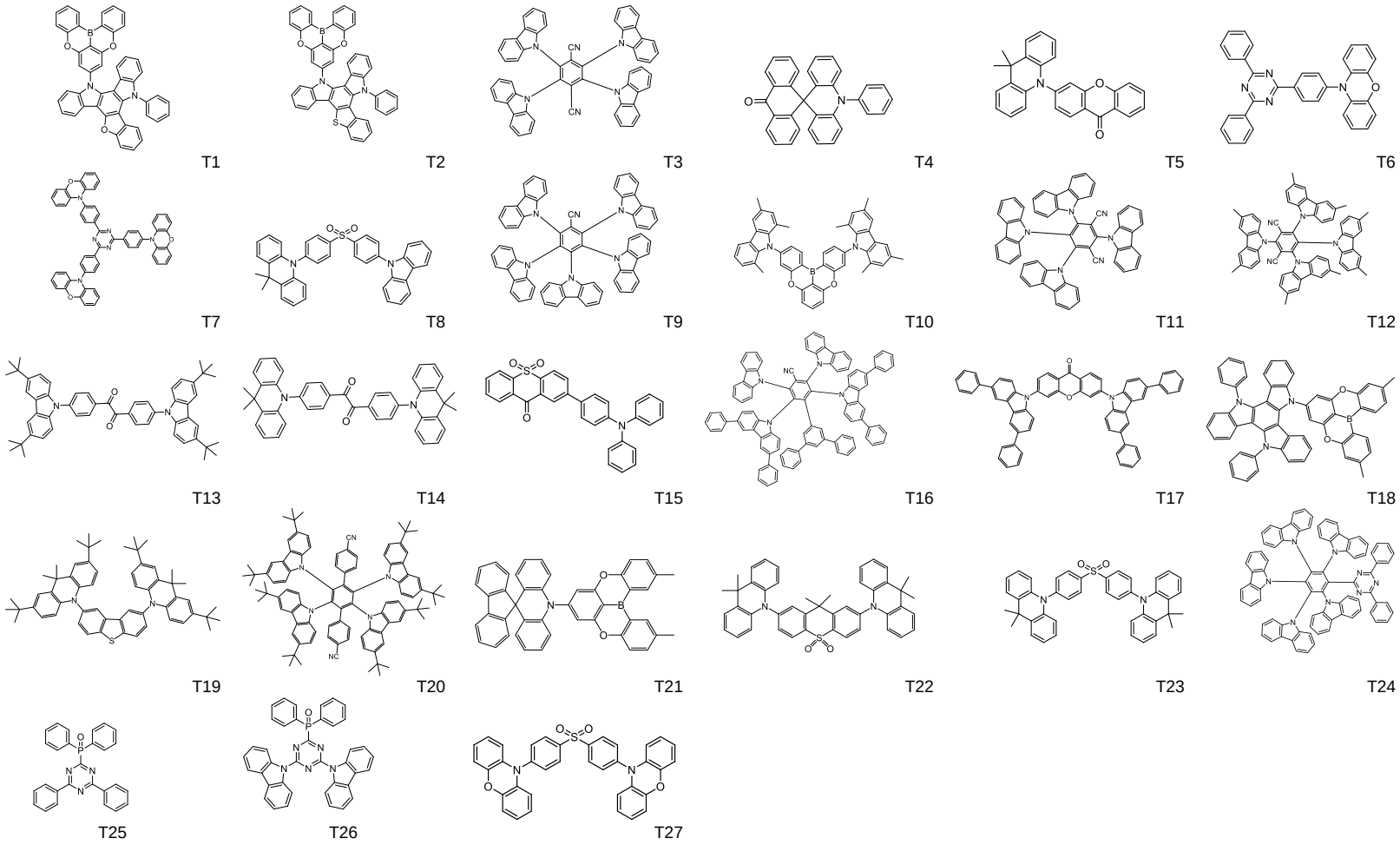

Fig. 4 Chemical structures of the TADF emitters.

maximum is placed at ~ 445 nm, which is close to the absorption of **F1**.[53] $\mathbf{T_1}$ and $\mathbf{T_2}$ also exhibit high Φ_{PL} of > 95% in pristine thin-films. The OLED active layer composition was prepared by mixing 25 wt % of $\mathbf{T_1}$ or $\mathbf{T_2}$ with 1 wt% of **F1** resulting in a high k_{FRET} of 7.50×10^7 and $7.48 \times 10^7\ s^{-1}$, respectively. These properties of the TADF/fluorescence emitter couple featured an efficient HF-OLED (see below).[53]

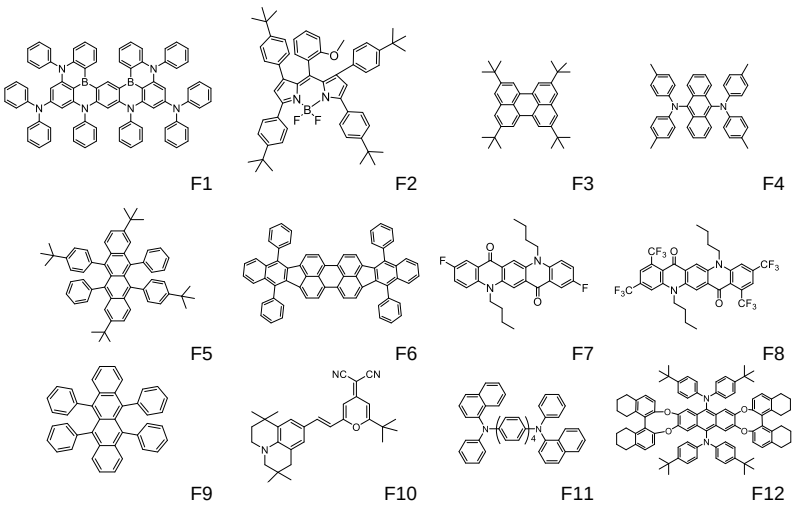

Fig. 5 Chemical structures of fluorescence emitters.

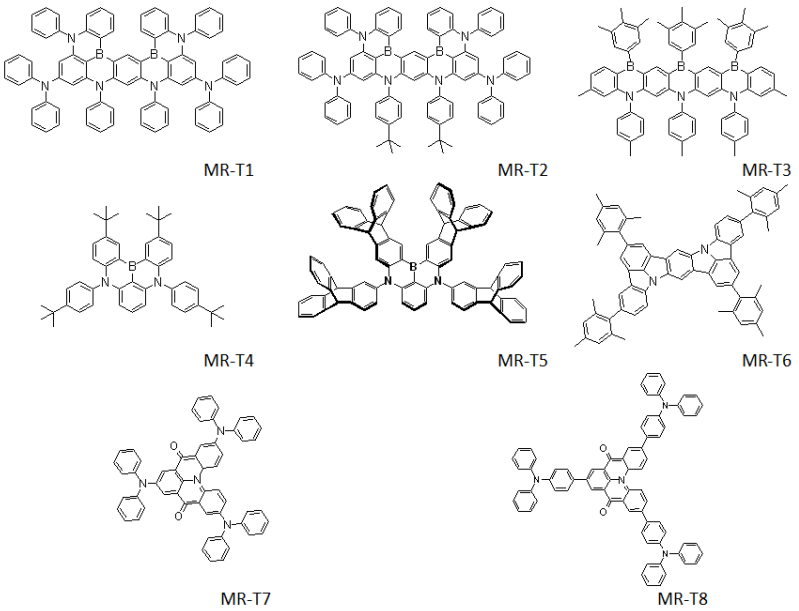

Fig. 6 Chemical structures of host materials.

Concerning the low-energy part of the visible spectrum, the Kwon group reported a red HF-OLED combining **F2** and a TADF emitter **T3** (**Figs. 4** and **5**).[57] Owing to the sharp emission and high Φ_{PL} of BODIPYs, they selected a BODIPY-based red emitting fluorescence emitter **F2** (emission maximum at 620 nm), featuring a high Φ_{PL} of 99% and a small FWHM of 31 nm in solution. However, the deep lowest unoccupied molecular orbital (LUMO) of 3.83 eV may induce electron trapping directly on BODIPY in the emissive layer. Therefore, a TADF emitter with deep LUMO would be best for these BODIPY-based fluorescence emitters, which help reduce the trapping of electrons in the emissive layer. Thus, they selected a TADF emitter **T3** (**Fig. 5**) that possesses a deep LUMO (3.9 eV) along with better spectral overlap with the absorption spectrum of **F2 and** the emission spectrum of **T3**. In addition, a high Φ_{PL} of 98% and high k_{FRET} of 5.10×10^7 s^{-1} were obtained for 0.7% doped films. Therefore, the selection of the **T3** and **F2** combination resulted in an efficient HF-OLED (see below).[57]

3. Hyperfluorescent OLEDs

There was a continuous success in designing HF-OLEDs after the first examples reported by the Adachi group.[49] Using a suitable host and the right choice of TADF-fluorescence emitter couple , such as **T4**:**F3**, **T5**:**F4**, **T6**:**F5**, and **T7**:**F6** (**Figs 3-5**), they succeeded to fabricating blue-, green-, yellow-, and red-emitting HF-OLEDs, respectively (**Table 1**).[49] With the limit of ~15-50 wt% doping concentrations of TADF emitters and 1 wt% of fluorescence emitter, the maximum EQE of the blue-, green-, yellow-, and red-emitting HF-OLEDs were 13.4%, 15.8%, 18.0%, and 17.5%, respectively.[49] There was a huge increase in EQE compared to conventional fluorescent emitters in all devices, demonstrating the EQE-enhancing role of HF emitters. No doubt, this approach demonstrates a path for designing several new HF emitters using theTADF-fluorescence emitter couple and their fruitful applications in OLEDs.[42-60]

However, a low EQE (13.4%) was observed for the first blue HF-OLED based on the **T4**:**F3** emitter couple (**Table 1**). This might be attributed to the incomplete FRET from the TADF emitter to the fluorescent emitter, as the TADF emitter (**T4**) emits at longer wavelength than the fluorescence emitter (**F3**), decreasing the spectral overlap J_F (eq. 4). In contrast, Lee group reported a HF-OLED showing improved EQEs, which contain a deep blue TADF emitter (**T8**) and fluorescence emitter (**F3**).[50] At 50 wt.% doping concentration of **T8** and 0.1 wt.% doping concentration of **F3**, a deep blue HF-OLED was fabricated with host **DPEPO** (**Table 1**). This resulted in an improved EQE reaching a value of 18.1%. These studies suggest that the choice of the **T8**:**F3** couple is better than the **T4**:**F3** couple for blue HF-OLED (**Figs. 4** and **5**). Further studies revealed that a blue HF-OLED constructed using a **T8**:**F3** couple without a host exhibits EQE of 15.4 %.[51] As the next steps, another TADF emitter **T9** was used to sensitize the blue emission of **F3**. Similar to the previous works, a solution-processed efficient blue HF-OLEDs was prepared, reaching an EQE of 18.8 % using a bulkier host **DPOBBPE** (**Table 1**).[52] These findings revealed that the nature of the host plays a vital role f in the device's performance by controlling Dexter energy transfer; the bulkier the host, the lesser will be the Dexter energy transfer. Kwon group recently developed two more blue-emitting TADF emitters, **T1** and **T2** (**Fig. 4**). Both emit deep blue emissions and exhibit high Φ_{PL}. HF-OLEDs were fabricated using **F1** as a dopant with host **DBFPO**.[53] The blue HF-OLEDs achieved using the **T1:F1** and **T2:F2** couple exhibit impressive EQE of 38.8% and 37.3%, respectively. In addition, the EL spectra of the both blue HF-OLEDs featured a FWHM of 19 nm.[53] Very recently Kwon group reported one blue HF-OLED using **T10** as quadrupolar donor-acceptor-donor type TADF emitter and **F1** as a fluorescence emitter in **DBFPO** host (**Fig. 3**) . The HF-OLED device fabricated with this combination exhibits high EQEs of 43.9% of with x/y CIE chromaticity coordinates of 0.12/0.16.[62] This significant increase was attributed to the successful control of the

DET process through efficient K_{RISC} and shielded LUMO in **T10**. In addition, the HF-OLED constructed using the **T10:F1** couple displays an EL peak maximum at 473 nm with a narrow FWHM of 21 nm.[62] These investigations suggest an efficient HF-OLED could be developed by the proper selection of host, TADF emitter, and fluorescence terminal emitter.

Besides blue HF-OLEDs, there were a few efforts to develop other (green, red, and white) HF-OLEDs (**Table 1**). In detail, an efficient green HF-OLED fabricated using TADF emitter **T11**, fluorescence emitters **F7** and **F8** with **mCP** host (**Figs. 3-5**).[54] The EQEs were 13.5% and 14.6% for **T11:F7** and **T11:F8** couple emitter, respectively. Here, it could be noted that, EQE of only ~5% was obtained using the traditional Alq3 host with TADF emitter **T11** and fluorescence emitters **F7** and **F8**.[54] This indicates the crucial role of the host towards high EQEs. Yellow HF-OLEDs with the TADF emitter **T12** and yellow emitting fluorescence emitter **F5** (**Figs. 4** and **5**), which feature a good overlap of the emission spectrum of **T12** with the absorption spectrum of **F5**, featured a maximum EQE of 19.1% using the **mCBP** host.[55] Finally, red HF-OLEDs were prepared mixing **T13** or **T14** with **F6** and **CBP** host.[56] The device composed of **T13:F6** exhibited a maximum EQE of 8 % and x/y CIE chromaticity coordinates of 0.61/0.38. The device performance with the **T14:F6** couple was lower than that of device with the **T13:F6**; this might be due to their different TADF behavior owing to the presence of different donor groups in **T13** and **T14**.[56] However, the EQE of the devices with **T13:F6** couple was higher than those with each component.[56] Recently, another red HF-OLED was reported using red-emitting BODIPY-based fluorescence emitter **F2** and TADF emitter **T3** (**Table 1**).[57]The fabricated HF-OLED with **T3** and **F2** shows EQEs of 19.4%. The device exhibits an EL peak maximum at 617 nm with x/y CIE chromaticity coordinates of 0.64/ 0.36 and a FWHM of 44 nm. In addition, the device shows a longer device lifetime of 954 h at 3000 cd m^{-2}.[57] Wang group reported a red HF-OLED using

TADF emitter **T15** and conventional red fluorescence emitter **F6** (**Table 1**). The HF-OLED fabricated using this combination resulted in a maximum EQE of 16.4% and x/y CIE chromaticity coordinates of 0.65/0.35.[65]

Recently, HF-OLEDs with MR-TADF materials as terminal emitters have been developed rapidly owing to their strong and narrow emission.[66-73] MR-TADF materials (**Fig. 6**) are fused polycyclic aromatic compounds with suitably placed electron-deficient and electron-rich centers, enabling their HOMO and LUMO separation on different atoms due to the opposite resonance/mesomeric effects.[74-76] This reduces ΔE_{ST} and triggers TADF emission. The rigid frameworks and short-range charge transfer features of MR-TADF materials make them ideal candidates for OLEDs realizing narrow emission with high color purity and high efficiency.[66-73]The following are some representative examples of this class of HF -OLEDs. Adachi group used TADF emitter **T16** to sensitize the narrow emission of MR-TADF emitter **MR-T1 (Figs. 4** and **6)**.[63] The presence of a bulky *m*-terphenyl (instead of carbazole) unit at the para-position of **T16** triggers a greenish-blue emission at ~ 475 nm in solution, which is close to the absorption maximum of MR**T1**, enabling efficient energy transfer between them. In thin film with 0.5 wt.% of **MR-T1** and 20 wt.% of **T16** the emission maximum observed at 485 nm with a Φ_{PL} of 86%. High k_{RISC} i.e., 9.2×10^5 s^{-1} in thin-film, attested an excellent TADF behavior. Moreover, a high FRET efficiency of about 64% from **T16** to **MR-T1**, indicates an efficient excited energy transfer from **T16** to **MRT1**. This combination resulted in an efficient narrow-emitting (FWHM = 19nm) HF-OLED with a maximum EQE of 41% and good stability (**Table 1**).[63] Zhang group reported a blue HF-OLED using the **T17: MR-T1** couple.[73] The donor-void-acceptor structural feature of **T17** justifies its high Φ_{PL} of 92% and displays an emission maximum at 440 nm in toluene. The HF-OLED fabricated with 30 wt% TADF sensitizer **T17** and 1 wt% MR-TADF emitter **MR-T1**, resulted in a maximum EQE of 20.6% with a narrow FWHM of 21 nm

that has x/y CIE chromaticity coordinates of 0.140/0.195.[73] In parallel, many researchers exploited B, N doped MR-TADF terminal emitters in HF-OLEDs to achieve narrow emission with high efficiencies and high color purity. Kwon group reported a modified MR-TADF emitter (**MR-T2**) by attaching the *tert*-butyl group to the **MR-T1** core.[67] As mentioned earlier, incorporating bulky groups into the backbone of the terminal emitter can effectively inhibit the DET process and increase Φ_{PL}. In thin film, **MR-T2** displayed a Φ_{PL} of 91.9%. This increase in Φ_{PL} compared to **MRT1** is due to the addition of the *tert*-butyl group. **MR-T2** showed a short delayed lifetime of 2.93 µs, and k_{RISC} of 2.54 × 10^5 s^{-1}. Therefore, they have selected a suitable TADF emitter, **T18** to sensitize the blue emission of the MR-TADF emitter, **MR-T2**.[67] The thin film obtained with 30 wt.% **T18** and 1% of **MR-T2** has a Φ_{PL} of 97.3% and a k_{FRET} of about 7.77× 10^7 s^{-1}. This indicates efficient energy transfer from **T18** to **MR-T2.** Therefore, the blue HF-OLED fabricated with the **MR-T2**:**T18** combination exhibits a maximum EQE of 40.7% along with a narrow FWHM of 19 nm and x/y CIE chromaticity coordinates of 0.12/0.15.[67] Zysman-Colman group reported a different B, N doped MR-TADF emitter, **MR-T3**. They have fabricated a HF-OLED using a **T19: MR-T3** couple with a **DPEPO** host, which has an EQE of 15% with a FWHM of 49 nm and x/y CIE chromaticity coordinates of 0.15/0.10.[48] Another blue HF device was fabricated based on TADF sensitizer **T20** and MR-TADF emitter **MR-T4** combination.[71] With an aim of developing an efficient TADF emitter, a sterically congested TADF emitter, **T20** with multiple donor groups was developed. The presence of multiple donor-acceptor moieties in the same molecule supported the orbital mixing of LE and CT states, ensuing a high k_{RISC} of 2.36 × 10^6 s^{-1}. Hence, the HF-OLED obtained with the **T20: MR-T4** combination records an EQE maximum of 32.5%, a FWHM of <30 nm and x/y CIE coordinates chromaticity of 0.13/0.12.[71] Very recently, the Lee group reported an MR-TADF emitter **MR-T5**, a sterically shielded and rigid emitter based on triptycene-fused B,N core. In doped film,

MR-T5 exhibits an emission maximum at 463 nm with a Φ_{PL} of 99%.[69] They have selected a suitable TADF emitter, **T21,** which effectively sensitizes the emission of **MR-T5**. The thin film with 20 wt% **T21** and 2 wt% **MR-T5** with **mCBP:DPEPO** exhibits a high k_{FRET} of about 4-6×10^7 s^{-1}. The HF-OLED with **T21: MR-T5** showed a maximum EQE of 27.5% and a FWHM of 29nm.[69] Moreover, the Zysman-Colman group reported a new acceptor-free MR-TADF molecule, **MR-T6**. **MR-T6** exhibits weak TADF with a Φ_{PL} of 67% and an emission maximum at 441 nm in 3 wt% PMMA film.[68]The HF device obtained with 35 wt% **T22** and 1 wt % **MR-T6**, reached a maximum EQE of 16.5%, with deep-blue x/y CIE chromaticity coordinates of 0.15/0.11.[68] Recently, same group reported green and red HF-OLEDs based on MR-TADF emitter **MR-T7** and **MR-T8**, respectively.[70] **MR-T7** with triphenylamine donor groups showed green emission at 551 nm with FWHM of 58 nm and Φ_{PL} of 93%, while **MR-T8** with diphenylamine donor groups showed a red emission at 617 nm with FWHM of 56 nm and Φ_{PL} of 60% in the 2 wt% **mCP** doped films. A green HF-OLED fabricated using 2 wt% **MR-T7** as emitter and 10wt% TADF sensitizer **T11**, recorded a high maximum EQE *o*f 30 % with x/y CIE chromaticity coordinates of 0.424/0.551. Also, a red HF OLED fabricated using 2wt% **MR-T8** as emitter and 10 wt% TADF sensitizer **T11** and recorded a high maximum EQE of 18% with x/y CIE chromaticity coordinates of 0.585/0.396 (**Table 1**).[70]

There is also increasing interest in designing novel organic-based emitters for the fabrication of white OLED (WOLED).[77-88]They are developed with low cost and have exhibited notable merits of high efficiency. The WOLED device is characterized by the x/y CIE coordinates of 0.33/0.33. Normally, white light is produced by the simultaneous blue, green, and red missions, or the addition of two complementary emissions.[58, 77-88] This is usually possible with organic emitters that exhibit dual/multiple/broad emissions.[78] In the case of HF-WOLEDs, the white light is obtained by combining the emissions of both TADF and fluorescence emitters, which covers the complete visible

range (400-800 nm).[89-99] **Fig. 7** depicts the co-emission mechanisms of the hyperfluorescent emitters to produce white light emission. Here, the TADF emitter performs a dual role, acting itself as a blue emitter and a sensitizer for fluorescence emitter. A HF-WOLED was developed with **T23** as blue TADF emitter, and **F5** as a yellow fluorescent emitter.[90]Both **T23** and **F6** (**Figs. 4** and **5**), were co-doped with 0.05% doping concentration, and the HF-WOLED device constructed in **DPEPO** host exhibits x/y CIE coordinates of 0.28/0.35 and high EQE of 15.5%.[90,91]Similarly, another HF-WOLED developed using a TADF emitter **T23** and orange-emitting rubrene (**F9**) without any host, reached EQEs of 7.48%. In addition, stable EL spectra were recorded with the change of the x/y CIE coordinates of 0.36/0.41 to 0.36/0.43 with increase in voltage from 5 V to 8 V.[94] Friend and coworkers reported a HF-WOLED by using a sky-blue TADF emitter **T24**, complemented by yellow and red emitting fluorescence emitters **F5** and **F1,** the device resulted in a high EQE of 21.8% with x/y CIE coordinates of 0.43/0.45.[98] Very recently, the Xu group reported an ultra-thin bilayer concept for the design of HF-WOLED, where a emissive layer contains an ultrathin layer of blue fluorescence emitter (**F3**), and a layer of TADF emitter (**T25** or **T26**) doped with a yellow fluorescence emitter (**F5**).[46] The efficiency of these HF-WOLEDs is highly sensitive to the thickness of the layers. At the thinness of 0.1nm of blue emitter layer, the device exhibits dual band EL spectra with x/y CIE coordinates of 0.40/0.50. The maximum EQE values of 20.9%, and 11.8 % are reported for the devices using TADF emitters **T25** and **T26**, respectively.[46] Similarly, the Tang group recently reported a HF-WOLED using a yellow emitter **F5** , blue emitter **F11** and a TADF emitter, **T6** with a pure hydrocarbon host, **SF4-TPE**.[99] They witnessed with an increase in thickness of the blue layer, the EL intensity becomes stronger and the HF-WOLED constructed using 10 nm thickness of the blue layer exhibited maximum EQE of 17.6% and x/y CIE coordinates of 0.39/0.39.[99]

Table 1. Details of active layer composition, HF-OLED performances (CE_{max}: Maximum current efficiency, PE_{max}: Maximum power efficiency); λ_{EL}: emission maxima of electroluminescence and FWHM: full width at half maximum.

Host	Composition of TADF (T): terminal emitter[a]	Device Performance					References
		λ_{EL}/FWHM (nm)	x/y CIE co-ordinates	EQE (%)	CE_{max} (cd A^{-1})	PE_{max} (lm W^{-1})	
DPEPO	15 wt% **T4**:1 wt% **F3**	-	0.17/0.30	13.4	27.0	18.0	(49)
mCP	50 wt% **T5**:1 wt% **F4**	-	0.29/0.59	15.8	45.0	47.0	(49)
mCBP	25 wt% **T6**:1 wt% **F5**	-	0.45/0.53	18.0	60	58	(49)
CBP	15 wt% **T7**:1 wt% **F6**	-	0.61/0.39	17.5	25	28	(49)
DPEPO	50 wt% **T8**:0.1 wt% **F3**	-	0.15/0.22	18.1	24.3	18.4	(50)
-	**T8**:0.3 wt% **F3**	-	0.15/0.23	15.4	23.7	23.4	(51)
DPOBBPE	25 wt% **T9**:1 wt% **F3**	-	0.14/0.20	18.8	29.1	14.3	(52)
DBFPO	25 wt% **T1**:1 wt% **F1**	473/19	0.12/0.15	38.8	30.0	-	(53)
DBFPO	25 wt% **T2**:1 wt% **F1**	473/19	0.12/0.15	37.3	28.3	-	(53)
DBFPO	30 wt% **T10**:1 wt% **F1**	473/21	0.12/0.16	43.9	36.6	-	(62)
mCP	**T11**:0.5 wt% **F7**	-	0.44/0.55	13.5	-	53.4	(54)
mCP	**T11**:0.5 wt% **F8**	-	0.44/0.54	14.6	-	46.1	(54)
mCBP	6.3 mol% **T12**:0.65 mol% **F5**	-	0.43/0.54	19.1	62	-	(55)
CBP	15 wt% **T13**:2 wt% **F6**	610, 666, 724	0.61/0.38	6.65	10.15	-	(55)
CBP	15 wt% **T14**:2 wt% **F6**	-	0.62/0.37	3.62	5.21	-	(56)
-	30 wt% **T3**:0.7 wt% **F2**	617/44	0.64/0.36	19.4	26.0	-	(57)
mCBP	25 wt% **T17**:1 wt% **F6**	610, 647, 710	0.65/0.33	21.5	27.4	-	(65)
mCBP	20 wt% **T16**:0.5 wt% **MR-T1**	470/19	0.13/0.16	41	23	72	(63)
mCP	30 wt% **T17**:1 wt% **MR-T1**	471/21	0.14/0.20	20.6	24.1	-	(73)
DBFPO	30 wt% **T18**:1 wt% **MR-T2**	474/19	0.12/ 0.15	40.7	31.6	-	(67)
DPEPO	25 vol% **T19**:1 vol% **MR-T3**	-/49	0.15/ 0.10	15	-	-	(48)
DPEPO	40 wt% **T20**: 2 wt% **MR-T4**	-/29	0.13/0.12	32.5	-	-	(71)
mCBP:DPEPO	20 wt% **T21**: 2 wt% **MR-T5**	462/29	0.14/ 0.13	27.5	28.5	29.8	(69)
DPEPO	35 wt% **T21**: 1 wt% **MR-T6**	-	0.15/0.11	16.5	-	-	(68)
mCP	10 wt% **T11**: 1 wt% **MR-T7**	556/70	0.42/0.55	30	106	111	(70)
mCP	10 wt% **T11**: 1 wt% **MR-T8**	615/61	0.56/0.40	17.9	35	37	(70)
-	10 wt% **T27**:1 wt% **(*S*,*S*)-F10**	536	-	21.5	72.1	69.8	(104)
-	10 wt% **T27**:1 wt% **(*R*,*R*)-F10**	536	-	20.4	67.9	68.2	(104)

[a] Terminal emitters are either fluorescence emitters (F) or MR-TADF emitters (MR-T)

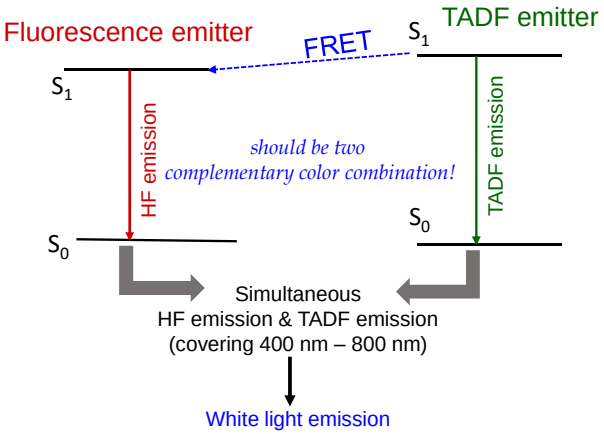

Fig. 7 Depicting the co-emission mechanism for white light emission with fluorescence emitter and TADF combination as hyperfluorescence mechanism.

Finally, there are a few more interesting examples with further features, such as circularly polarized electroluminescence.[100-103] Here, Chen et al. reported circularly polarized OLED based on hyperfluorescence mechanism.[93] In detail, they have used chiral fluorescence emitters (**F12**; **Fig. 5**) with $|g_{lum}|$ is about 2.5×10^{-3} and TADF sensitizer (**T27**; **Fig. 4**) in the active layer. The green HF-OLEDs fabricated using enantiomers (***S,S***)**-F10** and (***R,R***)**-F10** exhibit EQE of 21.5% and 20.4%, respectively.[104] Interestingly, these efficiencies of HF- OLEDs are much higher compared to reported fluorescence OLEDs.

4. Conclusion and future prospective

Significant advances in solid-state lighting technology have been made with the appealing use of new hyperfluorescent active layers and their respective OLEDs. Here, the Foster resonance energy transfer (FRET) between a TADF and fluorescent emitter plays a primary role in the device efficiency of blue-, green-, red- as well as white-emitting HF-OLEDs. In addition, circularly polarized HF-OLEDs using chiral emitters are also possible. In contrast to fluorescent OLEDs, all-hyperfluorescent OLEDs have high color purity (owing to their narrow emission) and significantly enhanced EQEs.

Today, there are still challenges/difficulties in the development of HF emitters and devices. For instance, the device lifetime is still limited, while the design of pure deep blue emitters is still necessary. To further improve the performance of HF-OLED, a twisted donor-acceptor based TADF emitter should be designed to achieve 100% triplet to singlet excitonic conversion by efficient reverse intersystem crossing. This might also reduce the use of high doping concentrations of TADF emitters. The efficient RISC and low doping concentration of TADF emitter will, in addition, help to avoid Dexter energy transfer from triplet excitons. In this line, the fluorescence emitters should be designed with sterically hindered bulky groups to minimize the Dexter energy transfer. In addition, Monkman group revealed that the rate of DET is very difficult to get from photophysical measurements in thin film.[105] Therefore, it is the biggest challenge to quantify rate of DET in thin film and hence a suitable technique should be developed for the calculation of DET rate in thin film. Moreover, the selection of suitable host materials for OLED is also a big challenge because it is very difficult to design high triplet energy host materials. In this context, the recent work of the Bryce group should be followed, which provides molecular design directions for obtaining very high triplet energy host materials.[106] Recently , it was observed that phosphine oxide-free hosts perform better in OLEDs and therefore, the design of new phosphine oxide-free hosts and their use in devices should be investigated.[107] Most of the reported MR-TADF emitter exhibits weak TADF emission and therefore, the design of efficient MR-TADF terminal emitters with high k_{RISC} is further required to have efficient HF-OLEDs. Finally, dyads based on covalent/non-covalent emitters could be explored; since they have the capacity to control distance towards an enhanced FRET process.

In the meantime, the design of HF-based light-emitting electrochemical cells (LECs) should be established.[108-110] LECs consist of a blend of an ion-electrolyte and an emitter in the active layer. Thus, combining Fluorescence/TADF based HF systems is feasible,

but the effect of the ion-induced local electric fields on the FRET and DET processes needs to be studied. Overall, we believe that HF emitters in solid-state lighting applications can achieve significant breakthroughs in efficiency and lifetime in the near future and therefore facilitate commercialization.

Conflicts of interest

There are no conflicts to declare.

Acknowledgements

Authors acknowledge PoTA-LEC, Grant # 101064004, funded by HORIZON-MSCA-2021-PF-01 of the European Commission.

References

1. G. Hong, X. Gan, C. Leonhardt, Z. Zhang, J. Seibert, J. M. Busch and S. Bräse, *Adv. Mater.*, 2021, **33**, 2005630.
2. S. S. Swayamprabha, D. K. Dubey, Shahnawaz, R. A. K. Yadav, M. R. Nagar, A. Sharma, F.-C. Tung and J.-H. Jou, *Adv.Sci.*, 2021, **8**, 2002254.
3. Y. Yin, M. U. Ali, W. Xie, H.Yang and H. Meng, *Mater. Chem. Front.*, 2019, **3**, 970.
4. F. Zhao and D. Ma, *Mater. Chem. Front.*, 2017, **1**, 1933.
5. H. Sasabe and J. Kido, *J. Mater. Chem. C*, 2013, **1**, 1699.
6. B. Song, W. Shao, J. Jung, S.-J. Yoon and J. Kim, *ACS Appl. Mater. Interfaces*, 2020, **12**, 6137.
7. J. Lee, H. F. Chen, T. Batagoda, C. Coburn, P. I. Djurovich, M. E. Thompson and S. R. Forrest, *Nat. Mater.*, 2015, **15**, 92.

8. C. Y. Kuei , W. L. Tsai , B. Tong , M. Jiao , W. K. Lee , Y. Chi and P. T. Chou, *Adv. Mater.*, 2016, **28** , 2795.
9. S.-J. Zou, Y. Shen, F.M. Xie, J.-D. Chen, Y.-Q. Li and J.-X. Tang, *Mater. Chem. Front.*, 2020, **4**, 788.
10. C. Murawski and M. C. Gather, *Adv.Opt. Mater.*, 2021, **9**, 2100269; Y. Huang, E.-L. Hsiang, M.-Y. Deng and S.-T. Wu, *Light Sci Appl*, 2020, **9**, 105.
11. Q. Wei, N. Fei, A. Islam, T. Lei, L. Hong, R. Peng, X. Fan, L. Chen, P. Gao and Z. Ge, *Adv. Opt. Mater*., 2018, **6**, 1800512.
12. Z. Yang, Z. Mao, Z. Xie, Y. Zhang, S. Liu, J. Zhao, J. Xu, Z. Chi and M. P. Aldred, *Chem. Soc. Rev.*, 2017, **46**, 915.
13. Y. Xiao, H. Wang, Z. Xie, M. Shen, R. Huang, Y. Miao, G. Liu, T. Yu and W. Huang, *Chem. Sci.*, 2022, **13**, 8906.
14. T. Huang, W. Jiangand L. Duan, *J. Mater. Chem. C*, 2018, **6**, 5577.
15. Y. Liu, C. Li, Z. Ren, S.Yan, M. R. Bryce, *Nat Rev Mater*., 2018, **3**, 18020.
16. Y.-Z. Shi, H. Wu, K.Wang, J. Yu, X.-M. Ou and X.-H. Zhang, *Chem. Sci.*, 2022, **13**, 3625.
17. H. Uoyama, K. Goushi, K. Shizu, H. Nomura and C. Adachi, *Nature*, 2012, **492** , 234.
18. M. Y. Wong and E. Zysman-Colman, *Adv. Mater.*, 2017, **29**, 1605444.
19. K. Goushi , K. Yoshida , K. Sato and C. Adachi, *Nat. Photonics*, 2012, **6**, 253.
20. X. Y. Cai and S. J. Su, *Adv. Funct. Mater.*, 2018, **28**, 1802558.
21. K. Liu, X.-L. Li, M. Liu, D. Chen, X. Cai, Y.-C. Wu, C.-C. Lo, A. Lien, Y. Cao, S.-J. Su, *J. Mater. Chem. C* 2015, **3**, 9999.
22. Q. Wei, Z.Ge and B. Voit, *Macromol. Rapid Commun*, 2019, **40**, 1800570.
23. G. Zhan, Z. Liu, Z. Bian and C. Huang, *Front. Chem.*, 2019, **7**, 305.

24. M. A. Baldo, D. F. O'Brien, Y. You, A. Shoustikov, S. Sibley, M. E. Thompson and S. R. Forrest, *Nature*, 1998, **395**, 151.
25. M. A. Baldo, M. E. Thompson and S. R. Forrest, *Pure Appl. Chem.*, 1999, **71**, 2095.
26. B. Minaev, G. Baryshnikov and H. Agren, *Phys. Chem. Chem. Phys.*, 2014, **16**, 1719.
27. K .R. Naveen, K. Prabhu CP, R . Braveenth and H. Kwon, *Chem.Eur. J.*, 2022, **28**, e2021035.
28. S. K. Behera, S. Y. Park and J. Gierschner, *Angew. Chem. Int. Ed.*, 2021, **60**, 22624.
29. Kenry, C. Chen and B. Liu, *Nat Commun*, 2019, **10**, 2111.
30. S. Mukherjee and P. Thilagar, *Chem. Comm.* 2015, **51**, 10988.
31. F. B Dias, T. J Penfold and A. P Monkman, *Methods Appl. Fluoresc.*, 2017, **5**, 012001.
32. S. K. Sarkar, M. Pegu, S. K. Behera, S. K. Narra and P. Thilagar, *Chemistry: An Asian Journal*, 2019, **14**, 4588.
33. S. Jena, J. Eyyathiyil, S.K. Behera, M. Kitahara, Y. Imai and P. Thilagar, *Chem Sci.*, 2022, **13**, 5893.
34. S. K. Behera, A. Karak and G. Krishnamoorthy, *J. Phys. Chem. B*, 2015, **119**, 2330.
35. S. K. Behera and G. Krishnamoorthy, *Photochemical & Photobiological Sciences* 2015, **14**, 2225.
36. J.-L. Renaud, S. Gaillard, G. U. Mahoro, R. D. Costa, J. Fernandez-Cestau and P. Coto, *Adv. Opt. Mater.* 2020, **8**, 2000260.
37. R. D. Costa, F. Monti, H. J. Bolink, E. Ortí, G. Accorsi and N. Armaroli, *Angew. Chem., Int. Ed.* 2012, **51**, 8178.
38. L. M. Cavinato, K. Yamaoka, S. Lipinski, V.Calvi, D. Wehenkel, R. v. Rijn, K. Albrecht and R. D. Costa, *Adv. Funct. Mater.*, 2023, 2302483.

39. S. Lipinski, L. M. Cavinato, T. Pickl, G. Biffi, A. Pöthig, P. B. Coto, J. Fernández-Cestau and R. D. Costa, *Adv. Optical Mater.,* 2023, 2203145.

40. E. C. Constable, M. Neuburger, P. Rösel, G. E. Schneider, J. A. Zampese, C. E. Housecroft, F. Monti, N. Armaroli and R.D. Costa and E. Ortí, *Inorg. Chem.,* 2013, **52**, *885.*

41. R. D. Costa, E. Ortí, D. Tordera, A. Pertegás, H. J. Bolink, S. Graber, C. E. Housecroft, L. Sachno, M. Neuburger and E. C. Constable, A*dv. Energy Mater., 2011***, 1,** 282.

42. H. Abroshan, Y. Zhang, X. Zhang, C. Fuentes-Hernandez, S. Barlow, V. Coropceanu, S. R. Marder, B. Kippelen and J.-L.Brédas, *Adv. Funct. Mater.*, 2020, **30**, 2005898.

43. S. Y.Byeon, D. R. Lee, K. S.Yook and J.Y. Lee, *Adv. Mater.* 2019, **31**, 1803714.

44. H. Abroshan, V. Coropceanu and J.-L. Bredas, *ACS Materials Lett.*, 2020, **2**, 1412.

45. E.Y. Park, J. H. Park, Y.-H. Kim and M. C. Suh, *J. Mater. Chem. C*, 2022, 10, 4705.

46. C. Duan, Y. Xin, Z. Wang, J. Zhang, C. Han and H. Xu, *Chem. Sci.*, 2022, **13**, 159.

47. A. Shahalizad, A. Malinge, L. Hu, G. Laflamme, L. Haeberlé, D. M. Myers, J. Mao, W.G. Skene and S. Kéna-Cohen, *Adv. Funct. Mater.*, 2021, **31**, 2007119.

48. K. Stavrou, S. M. Suresh, D. Hall, A. Danos, N. A. Kukhta, A. M. Z. Slawin, S. Warriner, D. Beljonne, Y. Olivier, A. Monkman and E. Zysman-Colman, *Adv. Opt. Mat.* 2022, **10**, 2200688.

49. H. Nakanotani, T. Higuchi, T. Furukawa, K. Masui, K. Morimoto, M. Numata, H. Tanaka, Y. Sagara, T. Yasuda and C. Adachi, *Nat. Commun.*, 2014, **5**, 4016.

50. I. Lee, W. Song, J. Y. Lee and S.-H. Hwang, *J. Mater. Chem. C*, 2015, **3**, 8834.

51. W. Song, I. Lee and J. Ye. Lee, *Adv. Mater.*, 2015, **27**, 4358.

52. S. K. Jeon, H.-J. Park and J. Y. Lee, *ACS Appl. Mater. Interfaces*, 2018, **10**, 5700.

53. R. Braveenth, H. Lee, J. D. Park, K. J. Yang, S. J. Hwang, K. R. Naveen, R. Lampande and J. H. Kwon, *Adv. Funct. Mater.*, 2021, **31**, 2105805

54. S. Wang, Y. Zhang, W. Chen, J. Wei, Y. Liu and Y, Wang, *Chem. Commun.*, 2015, **51**, 11972.

55. T. Furukawa, H. Nakanotani, M. Inoue and C. Adachi, *Sci. Rep.*, 2015, **5**, 8429.

56. D. J. Chen, X. Y. Cai, X. L. Li, Z. Z. He, C. S. Cai, D. C. Chen and S. J. Su, *J. Mater. Chem. C*, 2017, **5**, 5223.

57. Y. Hun Jung, D. Karthik, H. Lee, J. H. Maeng, K. J. Yang, S. Hwang and J. H. Kwon, *ACS Appl. Mater. Interfaces*, 2021, **13**, 17882.

58. W. Xie, X. Peng, M. Li, W. Qiu, W. Li, Q. Gu, Y. Jiao, Z. Chen, Y. Gan, K. k. Liu and S. J. Su, *Adv. Optical Mater.*, 2022, **10**, 2200665.

59. Y.-T.Lee, C.-Y. Chan, M. Tanaka, M. Mamada, K.Goushi, X. Tang, Y.Tsuchiya, H. Nakanotani and C. Adachi, *Adv. Optical Mater.* 2022, **10**, 2200682.

60. K. Stavrou, L. G. Franca, T. Böhmer, L. M. Duben, C. M. Marian and A. P. Monkman, *Adv. Funct. Mater.*, 2023, 2300910.

61. L. E. de Sousa, L. dos Santos Born, P. H. de Oliveira Neto and P. de Silva, *J. Mater. Chem. C*, 2022, **10**, 4914.

62. H. Lee, R. Braveenth, S. Muruganantham, C. Y. Jeon, H. S. Lee and J. H. Kwon, *Nature Commun.*, 2023, **14**, 419.

63. C.-Y. Chan, M. Tanaka, Y.-T. Lee, Y.-W. Wong, H. Nakanotani, T. Hatakeyama and C. Adachi, *Nat. Photonics*, 2021, 15, 203.

64. Y. Kondo, K. Yoshiura, S. Kitera, H. Nishi, S. Oda, H. Gotoh, Y. Sasada, M. Yanai and T. Hatakeyama, *Nat. Photonics* 2019, **13**, 678.

65. Z. Li, X. Hu, G. Liu, L. Tian, H. Gao, X. Dong, T. Gao, M. Cao, C.-S. Lee, P. Wang and Y. Wang, *J. Phys. Chem. C*, 2021, **125**, 1980.

66. Y. X. Hu, J. Miao, T. Hua, Z. Huang, Y. Qi, Y. Zou, Y. Qiu,

H. Xia, H. Liu, X. Cao and C. Yang, *Nat. Photon.*, 2022, **16**, 803.

67. K. R. Naveen, H.Lee, R. Braveenth, D. Karthik, K. J. Yang, S. J. Hwang, and J. H. Kwon, *Adv. Funct. Mater*., 2022, **32**, 2110356.
68. D. Hall,K. Stavrou, E. Duda, A.Danos, S. Bagnich, S. Warriner, A. M. Z. Slawin, D. Beljonne, A. Ko¨hler, A. Monkman,Y. Olivier and E. Zysman-Colman, *Mater. Horiz.*, 2022, **9**, 1068.
69. H. Mubarok, A. Amin, T. Lee, J. Jung, J.-H. Lee and M. H. Lee, *Angew. Chem. Int. Ed.*, 2023, **62**, e202306879.
70. S. Wu, A. K. Gupta, K. Yoshida, J.Gong, D.Hall, D.B. Cordes, A. M. Z. Slawin, I. D. W. Samuel and E. Zysman-Colman, *Angew. Chem. Int. Ed.*, 2022, **61**, e202213697.
71. D. Zhang, X. Song, A. J. Gillett, B. H. Drummond, S. T. E. Jones, G. Li, H. He, M. Cai, D. Credgington and L. Duan, *Adv. Mater*., 2020, **32**, 1908355.
72. Y. Zhang, D. Zhang,J. Wei, Z. Liu, Y. Lu and L. Duan, *Angew. Chem. Int. Ed.*, 2019, 58, 16912.
73. D. Zhang, Y. Wada, Q. Wang, H. Dai, T. Fan, G. Meng, J. Wei, Y. Zhang, K. Suzuki, G. Li, L. Duan and H. Kaji, *Adv. Sci.*, 2022, **9**, 2106018.
74. H. Hirai, K. Nakajima, S. Nakatsuka, K. Shiren, J. Ni, S. Nomura, T. Ikuta and T. Hatakeyama, *Angew.Chem.Int.Ed.,* 2015, **54**,13581.
75. S. Madayanad Suresh, D. Hall, D. Beljonne, Y.Olivier and E. Zysman-Colman, *Adv. Funct. Mater.*, 2020, **30**, 1908677.
76. H. Li, F. Xie, Y. Li and J. Tang, *J. Mater. Chem. C*, 2023,**11**, 6471.
77. H. Liu, Y. Fu, B. Z. Tang and Z. Zhao, *Nature Commun.*, 2022, **13**, 5154.
78. S.K. Behera, R. Kainda, S. Basu and Y. S. Chaudhary, *Appl. Mater. Today***,** 2022, **27**, 101407.

79. S. Park, J. E. Kwon, S. H. Kim, J. Seo, K. Chung, S. Y. Park, D. J. Jang, B. M. Medina, J. Gierschner and S. Y Park, *J. Am. Chem. Soc.* 2009, **131**, 1404.
80. K. T. Kamtekar, A. P. Monkman and M. R. Bryce, *Adv Mater.*, 2010, **22**, 572.
81. X. Wei, L.Gao, Y. Miao, Y. Zhao, M. Yin, H. Wang and B. Xu, *J. Mater. Chem. C*, 2020, **8**, 2772.
82. S. Mukherjee and P. Thilagar, *Dyes Pigm*. **2014**, 110, 2.
83. S. Su, E. Gonmori, H. Sasabe and J. Kido, *Adv. Mater.*, 2008, **20**, 4189.
84. M. Gather, A. Köhnen and K. Meerholz, *Adv. Mater.*, 2011, **23**, 233.
85. G. Farinola and R. Ragni, *Chem. Soc. Rev.*, 2011, **40** , 3467.
86. E. Fresta, J. Dosso, J. Cabanillas-González, D. Bonifazi and R. D. Costa, *Adv. Funct. Mater.*, 2020, **30**, 1906830.
87. C. Ezquerro, E. Fresta, E. Serrano, E. Lalinde, J. García-Martínez, J. R Berenguer and R. D. Costa, *Mater. Horiz.* 2019, **6**, 130.
88. E. Fresta, J. Fernández-Cestau and R. D. Costa, *Adv. Opt. Mater*, 2019, **7**, 1900830.
89. Z. Wang, X.-L. Li, Z. Ma, X.Cai, C.Cai, and S.-J. Su, *Adv. Funct. Mater*. 2018, 28, 1706922
90. W. Song, I. H. Lee, S.-H. Hwang and J. Y. Lee, *Org. Electron*, 2015, **23**, 138.
91. Z. B. Wu, L. Yu, F. C. Zhao, X. F. Qiao, J. S. Chen, F. Ni, C. L. Yang, T. Ahamad, S. M. Alshehri and D. G. Ma, *Adv. Opt. Mater.*, 2017, **5**, 1700415.
92. T. Higuchi, H. Nakanotani and C. Adachi, *Adv. Mater.* 2015, **27**, 2019.
93. Z. B. Wu, L. Yu, X. K. Zhou, Q. X. Guo, J. J. Luo, X. F. Qiao, D. Z. Yang, J. S. Chen, C. L. Yang and D. G. Ma, *Adv. Opt. Mater*. 2016, **4**, 1067.
94. B. Zhao, T. Zhang, W. Li, Z. Su, B. Chu, X. Yan, F. Jin, Y. Gao and H. Wu, *Org. Electron.*, 2015, **23**, 208.
95. T. Zhang, B. Zhao, B. Chu, W. Li, Z. Su, X. Yan, C. Liu, H. Wu, Y. Gao, F. Jin and F. Hou, *Sci. Rep.*, 2015, **5**, 10234.

96. M. I. Alam, M. R. Nagar, S. R. Nayak, A. Choudhury, J.-H. Jou and S.Vaidyanathan, *Adv. Optical Mater.,* 2022, **10**, 2200376.

97. F. Khan, E. Urbonas, D.Volyniuk, J. V. Grazulevicius, S. M. Mobin, and R. Misra, *J. Mater. Chem. C*, 2020, **8**, 13375.

98. L.-S. Cui, A. J. Gillett, S.-F. Zhang, H.Ye, Y. Liu, X.-K. Chen, Z.-S. Lin, E.W. Evans, W. K. Myers, T.K. Ronson, H. Nakanotani, S. Reineke, J.-L. Bredas, C. Adachi and R. H. Friend, *Nature Photonics*, 2020, **14**, 636.

99. X. Tang, Y. Li, Y.-K. Qu, C.-C. Peng, A. Khan, Z.-Q. Jiang and L.-S.Liao, A*dv. Funct. Mater.* 2020, **30**, 1910633.

100. Y.-P. Zhang, M.-X.Mao, S.-Q. Song, Y. Wang, Y.-X. Zheng, J. L. Zuo and Y. Pan, *Angew. Chem. Int. Ed.*, 2022, **61**, e202200290.

101. D.-W. Zhang, M. Li and C.-F. Chen, *Chem. Soc. Rev.*, 2020, **49**, 1331.

102. S. Feuillastre, M. Pauton, L. Gao, A. Desmarchelier, A. J. Riives, D. Prim, D. Tondelier, B. Geffroy, G. Muller, G. Clavier and G. Pieters, *J. Am. Chem. Soc.*, 2016, **138** , 3990.

103. S. Sun, J. Wang, L. Chen, R. Chen, J. Jin, C. Chen, S. Chen, G. Xie, C. Zheng and W. Huang, *J. Mater. Chem. C*, 2019, **7**, 14511.

104. M. Li, M.-Y. Wang, Y.-F. Wang, L. Feng and C.-F. Chen, *Angew. Chem. Int. Ed.*, 2021, **60**, 20728.

105. N. Haase, A. Danos, C. Pflumm, P. Stachelek, W. Brutting and A. P. Monkman, *Mater. Horiz.*, 2021, **8**, 1805.

106. I. A. Wright, A. Danos, S. Montanaro, A. S. Batsanov, A. P. Monkman, and M. R. Bryce, *Chem. Eur. J.*, 2021, **27**, 6545.

107. S.-G. Ihn, D. Jeong, E. S. Kwon, S. Kim, Y. S. Chung, M. Sim, J. Chwae, Y. Koishikawa, S. O. Jeon, J. S. Kim, J. Kim, S. Nam, I. Kim, S. Park, D. Sin Kim, H.Choi, and S. Kim, *Adv. Sci.,* 2022, **9**, 2102141

108. E. Fresta and R. D. Costa, *J. Mater. Chem. C*, 2017, **5**, 5643.

109. R. D. Costa, E. Ortí and H. J. Bolink, P*ure and Applied Chemistry* 2011, **83**, 2115.

110. E. Fresta, A. Charisiadis, L. M Cavinato, N. Palandjian, K. Karikis, V. Nikolaou, G. Charalambidis, A. G Coutsolelos and R. D. Costa, A*dv. Photonics Research,* 2021, ***2***, 2000188.